

# **Dual-Phase Cathodes for Metal-Supported Solid Oxide Fuel Cells: Processing, Performance, Durability**

D. Udomsilp, © <sup>1,2,z</sup> F. Thaler, <sup>1,2</sup> N. H. Menzler, © <sup>2,\*</sup> C. Bischof, <sup>1</sup> L. G. J. de Haart, <sup>2,\*</sup> A. K. Opitz, © <sup>1,3</sup> O. Guillon, <sup>2,4</sup> and M. Bram <sup>1,2</sup>

Cathode processing is one of the main challenges in the manufacturing of metal-supported solid oxide fuel cells (MSCs). Cathode sintering in ambient air is not applicable to MSCs, as oxidation of the metal substrate and the metallic Ni of the anode damages the cell. A recently developed ex situ sintering procedure for the LSCF cathode in an argon atmosphere was shown to significantly improve cathode adherence. However, the stability of the sintered cathode layer posed a challenge during storage in ambient air. In the present work, adapting the ex situ sintering approach to LSC/GDC dual-phase cathodes not only enabled the ex situ sintering process to be applied to LSC-based cathodes, but also resulted in the superior stability of the cathode after sintering. Despite the hygroscopic properties of the partially decomposed perovskite, LSC/GDC dual-phase cathodes were shown to withstand more than 1 year of storage in ambient air without failure. Electrochemical single-cell measurements and post-test analysis confirmed the reversibility of phase transformations and the electrochemical activity of such dual-phase cathodes. Current densities of 1.30 A cm<sup>-2</sup> at 750°C, 0.85 A cm<sup>-2</sup> at 700°C, and 0.54 A cm<sup>-2</sup> at 650°C were obtained at a cell voltage of 0.7 V.

© The Author(s) 2019. Published by ECS. This is an open access article distributed under the terms of the Creative Commons Attribution 4.0 License (CC BY, http://creativecommons.org/licenses/by/4.0/), which permits unrestricted reuse of the work in any medium, provided the original work is properly cited. [DOI: 10.1149/2.0561908jes]

Manuscript submitted March 18, 2019; revised manuscript received April 17, 2019. Published April 30, 2019.

Solid oxide fuel cells (SOFCs) are electrochemical energy converters that directly convert chemical energy stored in fuels into electrical energy. This direct conversion yields high efficiencies, both electrical and total, especially if combined with excess heat utilization in combined heat and power plants. The high operating temperature of SOFCs enables fuel flexibility, for instance using hydrogen as well as reformates from methane, ethanol, or diesel. SOFC power generators might therefore use existing infrastructure during the transition period from a power supply based on fossil fuels to one based on renewables. Moreover, the direct conversion facilitates silent operation, as the intermediate conversion steps of thermal energy and mechanical energy to electrical energy can be omitted. Therefore, no moving parts are present in an SOFC. These properties make SOFCs a promising technology for contributing substantially to the clean power supply of prospective energy systems. <sup>1-4</sup>

Metal-supported fuel cells (MSCs) utilizing a porous metal for mechanical support were developed in various institutions.<sup>5–12</sup> The anticipated improvement in robustness for these types of cells with respect to thermal cycles, vibrations, and redox stability is an important prerequisite for use in mobile applications, where short start-up times, cyclic operation, and higher mechanical loads are inevitable. Whereas initial approaches were aimed at utilizing MSCs in auxiliary power units (APUs) for heavy-duty vehicles (e.g. those developed by AVL List GmbH, Graz, Austria), recent attempts have included their application as a range extender for battery electric vehicles (AVL List GmbH; Nissan Motors Co. Ltd., Japan). 11,13 Since 2008, Plansee SE (PSE, Reutte, Austria) has developed an MSC concept based on its ITM (intermediate temperature metal) oxide-dispersion-strengthened ferritic steel support in close cooperation with Forschungszentrum Jülich GmbH (Jülich, Germany). 14-18 While the fabrication of anode, electrolyte, and diffusion barrier layers (DBLs) can be adapted to applications on the metal substrate, a separate cathode sintering step has not yet been implemented in the state-of-the-art process. This is due to the contradicting requirements of the metal substrate and the cathode with regard to the sintering atmosphere. Whereas the metal substrate must be sintered in a reducing atmosphere, cathode sintering is typically performed in oxidizing conditions. Hence, in situ activation by feeding air to the cathode side after sealing the gas compartments or

the infiltration of pre-sintered ceramic backbone structures are commonly used for cathode fabrication. These procedures are, however, restricted in terms of the adherence of in-situ-activated cathodes to the electrolyte or the performance degradation of infiltrated cathodes due to the coarsening of fine catalyst particles. <sup>6,19</sup>

Recently, an ex situ sintering procedure was developed for LSCF cathodes. 14,20-22 The sintering of entire cells in argon at 950°C clearly improved cathode adherence. At the same time, detrimental oxidation of the metal support and the Ni in the anode was prevented reliably. Partial phase decomposition of the perovskite cathode material, caused by sintering in a low  $p(O_2)$  atmosphere, was found to be reversible upon heating in ambient air during the first hours of cell operation. Single-cell testing of cells with such cathodes sintered ex situ did not reveal a detrimental effect on cell performance. Nevertheless, the formation of small amounts of La2O3 during sintering was found to be critical with regard to layer stability, if stored under ambient conditions between sintering and operation. Within several days, the reaction of La<sub>2</sub>O<sub>3</sub> with humidity from ambient air to form La(OH)<sub>3</sub> resulted in the detachment of the cathode layer due to significant volume expansion associated with hydroxide formation. Encapsulation of the sintered cell in a foil pouch prevents exposure to humidity, thereby extending the tolerable time between sintering and testing of the cell.<sup>14,21</sup> In an industrial environment, storage might be enabled by using a dry room. Nonetheless, this procedure complicates the long-term storage and handling of cells. Optimized fabrication aiming to enhance the reliability of cathode layers is therefore favorable. This paper reports on the recent progress achieved by applying LSC/GDC dual-phase cathodes sintered ex situ on MSCs.

## **Experimental**

MSC half-cells, i.e. cells without a cathode layer, were fabricated and provided by PSE. The substrate was prepared by powder metallurgy, starting with mechanically alloyed ITM (Fe-26Cr, Mo, Ti) powder. Tape casting and sintering was used for substrate fabrication.  $^{23,24}$  A Ce<sub>0.8</sub>Gd<sub>0.2</sub>O<sub>2- $\delta$ </sub> (gadolinium-doped ceria – GDC) diffusion barrier layer (DBL) was applied on the ITM support by magnetron sputtering – a physical vapor deposition (PVD) process – in order to prevent the interdiffusion of Fe/Cr from the substrate and Ni from the anode. The Ni/YSZ (Zr<sub>0.85</sub>Y<sub>0.15</sub>O<sub>2- $\delta$ </sub> – yttria-stabilized zirconia (YSZ)) cermet anode was produced by screen printing and sintering. A graded 3-layer structure was applied in order to cover the coarse substrate

 $<sup>^{</sup>l}$  Christian Doppler Laboratory for Interfaces in Metal-Supported Electrochemical Energy Converters, Jülich, Germany

<sup>&</sup>lt;sup>2</sup>Forschungszentrum Jülich GmbH, Institute of Energy and Climate Research, 52425 Jülich, Germany

<sup>&</sup>lt;sup>3</sup>TU Wien, Institute of Chemical Technologies and Analytics, 1060 Vienna, Austria

<sup>&</sup>lt;sup>4</sup> Jülich Aachen Research Alliance: JARA-ENERGY Jülich, Germany

<sup>\*</sup>Electrochemical Society Member.

<sup>&</sup>lt;sup>z</sup>E-mail: d.udomsilp@fz-juelich.de

surface and obtain a smooth surface for the subsequent electrolyte coating. The YSZ electrolyte was applied by gas flow sputtering and a second GDC DBL was deposited by magnetron sputtering to prevent the formation of zirconate phases between the electrolyte and cathode. Finally, the cathode was screen-printed to prepare the full-cell. Single phase  $La_{0.58}Sr_{0.4}Co_{1-x}Fe_xO_{3-\delta}$  (LSF: x = 1; LSCF: x = 0.8; LSC: x = 0) and dual-phase  $La_{0.58}Sr_{0.4}CoO_{3-\delta}/Ce_{0.8}Gd_{0.2}O_{2-\delta}$  (LSC/GDC) powders were used as cathode materials. Perovskite powders with a  $d_{50}$  of  $0.8 \pm 0.1$   $\mu m$  were prepared in-house by spray drying. For the experiments on dual-phase cathodes, the fabrication was based on the use of commercial GDC powder ( $d_{50}=0.25~\mu m$ , Treibacher Industrie AG, Austria). Different cathode materials were investigated as an alternative to LSCF in order to improve the reliability and storage capability of cells with cathodes sintered ex situ. LSF was chosen as a potentially more stable perovskite composition compared to LSCF and LSC. 25-29 Moreover, dual-phase compositions of the perovskites with GDC were prepared in order to improve the stability and reliability of the cathode. This effect is expected to result from i) the formation of a mechanically supporting GDC network, preventing delamination of the decomposed perovskite layer, or ii) reduction of the thermal expansion of the (dual-phase) cathode layer, which reduces the stress level in the sintered layer. Details of the cell preparation are reported elsewhere.<sup>30–33</sup> In addition, model samples were prepared by coating YSZ electrolyte substrates ( $25 \times 25 \text{ cm}^2$ ,  $200 \mu \text{m}$  thickness, Kerafol, Germany) with a GDC barrier layer by PVD and screen printing the cathode. These samples were sintered in a reducing atmosphere for a preliminary investigation of decomposition behavior and the mechanical stability of cathode layers.

The sintering of model samples and entire cells was performed in a tube furnace (RS 80/750/11, Nabertherm, Germany). During the sintering of MSCs, Ar(5.0) with 99.999% purity was fed at a flow rate of 840 sccm in order to protect the metal substrate from oxidation. Model samples with cathodes on electrolyte substrates were sintered in an Ar/2.9%H<sub>2</sub> (Ar/H<sub>2</sub>) atmosphere to simulate the influence of the porous metal on the p(O<sub>2</sub>) during thermal treatment. In previous experiments, this influence was identified by measuring the  $p(O_2)$  in the exhaust of the furnace. Pure Ar contains < 2 ppm residual oxygen (i.e.  $p(O_2) < 2 \, \cdot \, 10^{-6}$  bar). Due to a gettering effect of the porous metal, the  $p(O_2)$  was lowered to  $10^{-13}$  bar during the sintering of MSCs, depending on temperature, flow rate, and number of cells sintered simultaneously. The more reducing Ar/H<sub>2</sub> atmosphere (p(O<sub>2</sub>)  $\approx$ 10<sup>-20</sup> bar) was therefore chosen for model samples to process cathode layers under even more challenging conditions. Furthermore, the Ar/H<sub>2</sub> gas mixture provides a stable p(O<sub>2</sub>) during thermal treatment with good reproducibility. Re-oxidation of the partially decomposed cathodes was performed under thermal treatment at T > 800°C for 3 h in ambient air (model samples) or under air flow during cell operation (MSCs).

After sintering, the phase composition of the manufactured cathode layers was analyzed by X-ray diffraction (XRD, D4 Endeavor, Bruker Corp., USA, and Empyrean, PANalytical GmbH, Germany). The reversibility of phase decomposition was investigated by XRD analysis of re-oxidized cathodes, both for model samples and tested cells.

Single-cell testing at JÜLICH was performed on  $50 \times 50$  mm² cells with a 16 cm² active cathode area using a commercially available test rig from EBZ GmbH (Dresden, Germany) with a channel design flow field, in order to ensure a stable gas supply over the entire active area. Dry  $H_2$  was fed as fuel at a flow rate of 1000 sccm, with ambient air as an oxidant at 2000 sccm. Taking into account the maximum current density of 2 A cm $^{-2}$  (total current limited to 32 A by the test rig), these flow rates ensure a maximum fuel utilization of 22%. Therefore, no concentration limitation is expected during electrochemical characterization. Cells were sealed between two thin YSZ frames at  $850^{\circ}$ C using a glass sealant developed at ZEA-1 (Forschungszentrum Jülich). A Ni mesh was used as the anode contact and a Pt mesh as the cathode current collector. I-V curves were recorded at intervals of 50 K between  $850^{\circ}$ C and  $650^{\circ}$ C. The current density was increased in steps of 1.2 A min $^{-1}$  until the maximum current of 32 A,

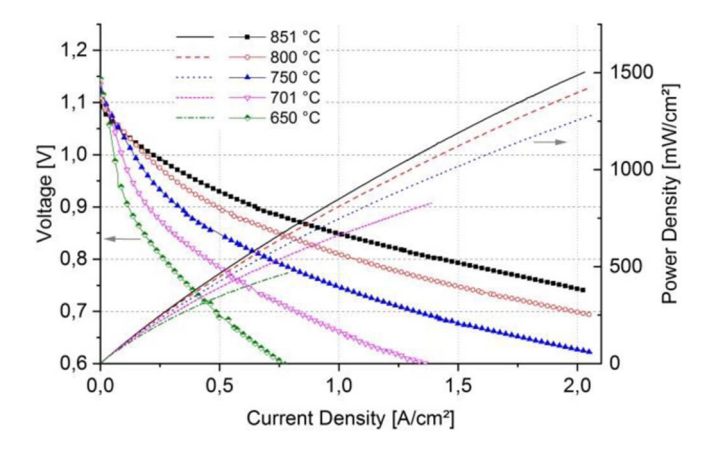


**Figure 1.** Reference I – I-V characteristics of an MSC with an LSCF cathode sintered ex situ at 950°C. Cell dimensions:  $50 \times 50 \text{ mm}^2$  with a  $16 \text{ cm}^2$  active cathode area. Gas supply:  $63 \text{ ml min}^{-1} \text{ cm}^{-2} \text{ H}_2$ ,  $125 \text{ ml min}^{-1} \text{ cm}^{-2}$  air.

or the minimum cell voltage of 0.6 V, was reached. Our previous work found that LSCF cathodes sintered ex situ on MSCs and re-oxidized during operation perform well and exhibit improved adhesion to the electrolyte compared to cathodes fabricated by the usual in situ activation procedure. <sup>14,21</sup> In the present investigation, new test benches and increased gas flow rates were used. Therefore, a cell with an LSCF cathode sintered ex situ was first tested electrochemically as a reference.

Single-cell testing at PSE was performed on button cells with a 35 mm diameter and a  $3.14\,\mathrm{cm^2}$  active cathode area. Dry  $H_2$  was fed at a flow rate of 200 sccm, resulting in an identical area-specific fuel supply rate of 63 ml cm $^{-2}$  min $^{-1}$  as was supplied at JÜLICH. Air was supplied at 600 sccm, as was the case in previous experiments.  $^{14}$  Both gases were supplied through alumina tubes perpendicular to the cell. Porous, 3-D-printed alumina stamps and zirconia felts were placed between the tubes and the meshes (anode - Ni, cathode - Au) contacting the cell, in order to provide reliable contact and homogeneous distribution of fuel and air.  $^{16}$ 

Post-test analysis was performed by SEM cross-sectional imaging (Ultra 55, Zeiss, Germany).

# **Results and Discussion**

Single-phase cathodes.—In order to investigate whether LSF provides improved thermochemical stability compared to LSCF, LSF cathode layers were printed on electrolyte substrates and sintered at 950°C in an Ar/H<sub>2</sub> atmosphere. Strong decomposition of the perovskite phase was observed by XRD, similar to results previously obtained for LSCF. Moreover, the failure of the sintered cathode layer by spallation occurred within several days, as had been reported earlier for LSC and LSCF.<sup>14</sup> It was therefore shown that LSF does not provide a significant improvement of phase stability and storage capability with regard to ex situ sintering. It can thus be concluded that none of the investigated La<sub>0.58</sub>Sr<sub>0.4</sub>Co<sub>1-x</sub>Fe<sub>x</sub>O<sub>3-δ</sub> perovskite compositions are stable in the long term under ambient conditions after ex situ sintering in an argon atmosphere. As a consequence, LSF was not considered for further experiments, as it is commonly regarded as a lower performing cathode material compared to LSCF. This means that LSCF is the only remaining pure perovskite material for ex situ sintering, as LSC was disregarded in our previous work<sup>14</sup> due to its low thermochemical stability. Nonetheless, LSC was considered for conventional in situ activation in order to make use of its high electrochemical performance and to compare the performance of cathodes sintered ex situ.

In Figure 1, reference I shows the I-V curves of a cell with an LSCF cathode sintered ex situ and measured at operating temperatures between 850°C and 650°C. The substantially higher performance compared to nominally identical cells published earlier<sup>14</sup> is related to the

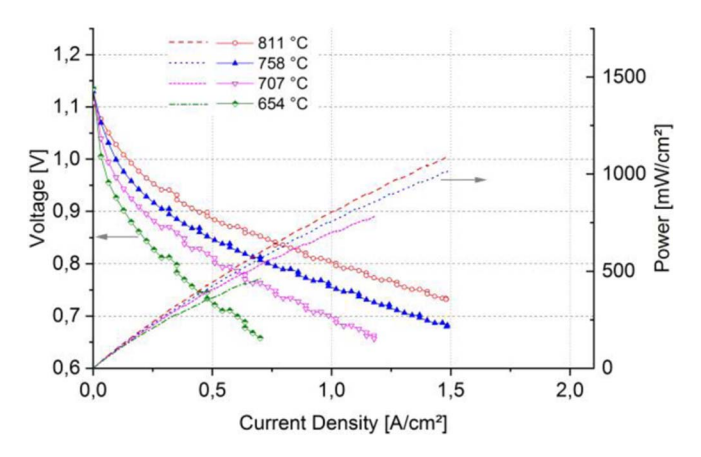


**Figure 2.** Reference II – I-V characteristics of an MSC button cell with an LSC cathode activated in situ during operation at 850°C. Cell dimensions:  $35 \text{ mm } \emptyset$  with a  $3.14 \text{ cm}^2$  active cathode area. Gas supply:  $63 \text{ ml min}^{-1} \text{ cm}^{-2}$  H<sub>2</sub>, 190 ml min<sup>-1</sup> cm<sup>-2</sup> air.

increased fuel and air supply in the present tests. Furthermore, an improved sealing procedure in the new test rig provides a higher OCV and might also contribute to improved performance. The current density of 1.32 A cm<sup>-2</sup> obtained at 0.7 V and 750°C corresponds well with the performance of button cells tested at Plansee, almost reaching the value of 1.37 A cm<sup>-2</sup> achieved with an LSC cathode activated in situ, which is shown in Figure 2 reference II. Due to the identical area specific fuel supply rates, these current densities correspond to fuel utilizations of 15% for both cells, which is sufficiently low to avoid gas conversion polarization. Using LSC as a cathode material, enhanced performance was achieved at a lower temperature, resulting in 0.99 A cm<sup>-2</sup> at 700°C and 0.60 A cm<sup>-2</sup> at 650°C.

**Dual-phase cathodes.**—A substantial improvement of cathode layer stability was achieved by utilizing dual-phase materials. Proof-of-concept was achieved on LSC/GDC cathodes, which were sintered on electrolyte substrates at 950°C under Ar/H<sub>2</sub> conditions for 3 h. It was found that the cathodes do not fail, even when stored in ambient air. As LSC is known to provide the highest electrochemical performance compared to LSF and LSCF, a further investigation was conducted on LSC/GDC (60/40 wt.-%) dual-phase cathodes. LSC/GDC (20 × 20 mm²) printed on a small MSC sample (25 × 25 mm²) was sintered under ex situ conditions (950°C, 3 h, Ar). No mechanical failure was observed during one year of storage. This is a very promising result, as it simplifies the handling of cells after ex situ sintering and enables larger time frames between sintering and operation.

The XRD analysis presented in Figure 3a reveals a pronounced phase decomposition of LSC after ex situ sintering, including the formation of La<sub>2</sub>O<sub>3</sub> and La(OH)<sub>3</sub>. The formation of Sr<sub>2</sub>CeO<sub>4</sub> indicates interaction between the LSC and GDC during thermal treatment in a low  $p(O_2)$  atmosphere. Figure 3b shows the XRD result after cell operation – i.e. after oxidative heat-treatment ( $T \ge 750^{\circ}$ C) of the decomposed cathode. From the observed peaks, the phase composition can be identified as GDC and LSC. Accordingly, a fully reversible

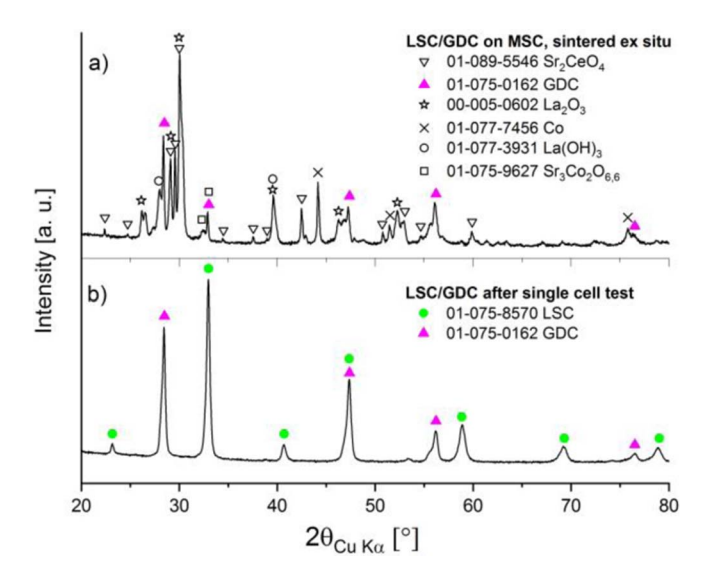


**Figure 3.** XRD analysis of an LSC/GDC cathode on an MSC a) sintered ex situ and b) after re-oxidation during cell operation (only the main diffraction peaks are indexed).

phase transformation (within the accuracy range of the XRD technique) occurred during cell operation.

Cell testing was performed at JÜLICH using the same procedure applied to the cell with an LSCF cathode. Figure 4 shows the I-V curves measured between 850°C and 650°C. The achieved performance, 1.30 A cm<sup>-2</sup> at 0.7 V and 750°C, is in the same range as previously observed with an LSCF cathode sintered ex situ (reference I). At higher temperatures, the performance of the dual-phase cathode is slightly lower, whereas at lower temperatures, cell

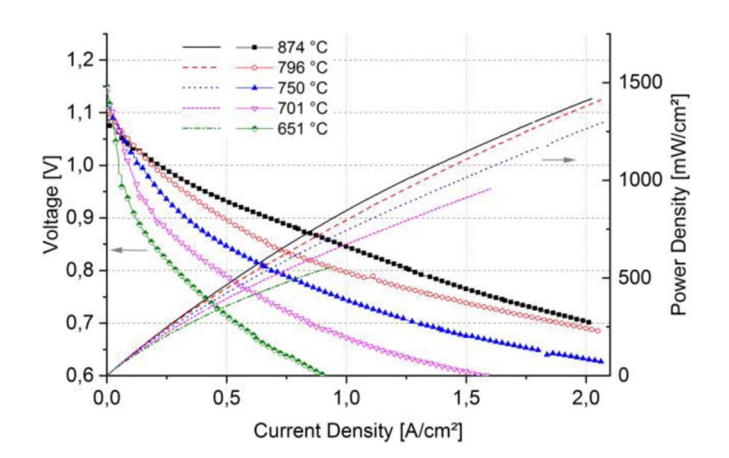


**Figure 4.** I-V characteristics of an MSC with an LSC/GDC cathode sintered ex situ at 950°C. Cell dimensions:  $50 \times 50 \text{ mm}^2$  with a 16 cm² active cathode area. Gas supply:  $63 \text{ ml min}^{-1} \text{ cm}^{-2} \text{ H}_2$ ,  $125 \text{ ml min}^{-1} \text{ cm}^{-2}$  air.

Table I. Comparison of the electrochemical performance of MSCs with an LSCF and LSC/GDC cathode sintered ex situ and an LSC cathode activated in situ.

Reference I LSCF cathode sintered ex situ			LSC/GDC cathode sintered ex situ			Reference II LSC cathode activated in situ		
T [°C]	OCV [V]	j @ 0.7 V [A cm <sup>-2</sup> ]	T [°C]	OCV [V]	j @ 0.7 V [A cm <sup>-2</sup> ]	T [°C]	OCV [V]	j @ 0.7 V [A cm <sup>-2</sup> ]
851	1.09	2.03 @ 0.74 V	874	1.09	2.02	-	-	-
800	1.11	1.99	796	1.11	1.90	811	1.11	1.48 @ 0.73 V
750	1.12	1.32	750	1.13	1.30	758	1.13	1.37
701	1.14	0.82	701	1.14	0.85	707	1.13	0.99
650	1.15	0.49	651	1.15	0.54	654	1.14	0.60

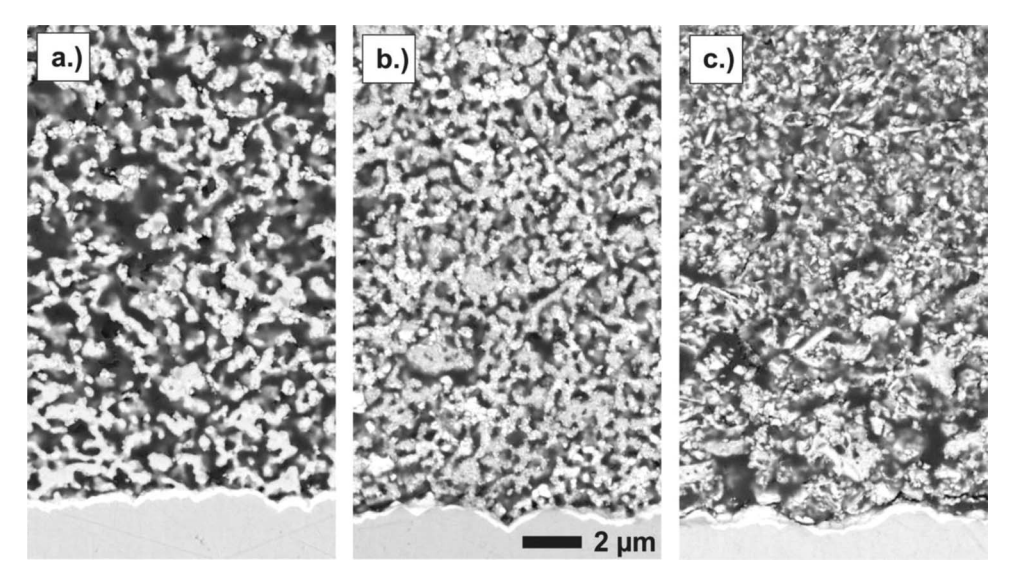


Figure 5. Cathode microstructure after single cell testing. a) LSCF cathode, b) LSC/GDC cathode, both sintered ex situ and re-oxidized during cell operation, and c) LSC cathode activated in situ.

performance is somewhat higher compared to LSCF but lower than pure LSC activated in situ (reference II), as summarized in Table I. The result confirms the applicability of ex situ sintering to perovskite/GDC dual-phase cathodes. Similar to pure LSCF cathodes, the electrochemical performance of the dual-phase material is restored during re-oxidation by reversible phase transformation. The performance on the same level as pure LSCF demonstrates the high potential of the dual-phase cathode, as the microstructure has not yet been optimized. Optimization of the microstructure is expected to bring about a further enhancement of performance by adjusting the particle size, perovskite/GDC ratio, and sintering conditions. However, at the current state of development, LSC cathodes activated in situ still appear to be the best choice in terms of high-performance MSC applications, especially when targeting at low operation temperatures.

Microstructural post-test analysis of the cells by SEM on polished cross sections is shown in Figure 5. The microstructure of the LSC/GDC cathode (Figure 5b) appears to be slightly finer and denser compared to the LSCF (Figure 5a). Both phases – perovskite and GDC - are homogeneously distributed in the dual-phase cathode layer. The LSC cathode (Figure 5c) exhibits the finest microstructure due to its lower activation temperature of 850°C compared to the ex situ sintering temperature of 950°C. These finer structures contribute to enhanced performance at low operation temperatures because of the larger active surface. In general, grain size, pore size, and their volume fractions are important parameters for the electrochemical activity of a cathode. These parameters, in turn, depend on the cathode composition as well as on the temperature of thermal treatment. Therefore, similar processing conditions do not necessarily result in similar microstructures for different materials.<sup>29,35</sup> The present work focuses on demonstrating the suitability of novel cathode concepts for MSCs and discusses the advantages and disadvantages of these concepts in a more general way. More detailed microstructural analysis and optimization will be the topic of future investigation. As the applicable sintering temperature range is rather narrow for the present MSC setup, adaptation of the composition and particle sizes present the greatest flexibility for improving the cathode design. The relatively small differences in performance between the different cathodes are expected to become even larger for Ni/GDC containing cells since the latter was shown to significantly improve cell performance thus increasing the influence of the cathode. The investigation of durability of such cells in long-term tests is subject of ongoing work, which will shed more light on stability of cathodes and anodes as well as interdiffusion and oxidation phenomena. Preliminary results show stable performance over

>700 h of continuous operation at 0.3 A cm $^{-2}$  and 700°C with H $_2$  as fuel and air as oxidant, indicating sufficient stability of the investigated cathodes.

A comparison of the achieved MSC performance to those of other MSC concepts is difficult to project for the cathode properties, as different cell setups and their specific properties must be considered. Well-established concepts include those of LBNL (USA), DTU (Denmark), and Ceres Power (UK), which conducted research on MSCs for more than one decade. All of these concepts utilize Ni and doped ceria as an active anode material, which provides higher electrochemical performance compared to Ni/YSZ, as was previously shown in PSE MSCs. 16,18 LBNL uses the infiltration of catalyst precursors into porous backbones for both the anode and cathode. Whereas most publications report on LSM as an active cathode material achieving 1.5 A cm<sup>-2</sup> at 0.7 V and 700°C, <sup>19</sup> it was recently reported that Pr<sub>6</sub>O<sub>11</sub> provided a superior performance of about 2.1 A cm<sup>-2</sup> under the same conditions.<sup>36</sup> The coarsening of infiltrated catalyst particles is expected to be the main degradation mechanism of these cells. DTU also applies an infiltrated anode design combined with the in situ activation of screen-printed (La,Sr)(Co,Fe)O<sub>3-δ</sub> cathodes, or composites thereof with GDC. Besides a performance of 1.3 A cm<sup>-2</sup> at 0.7 V and 700°C,<sup>37</sup> challenges regarding cathode delamination were reported.<sup>9</sup> Ceres Power is the only institution reporting cathode sintering in air (no temperature reported) before cell operation. Their specific cell design aims at a low operation temperature of  $\leq 600^{\circ}$ C, as it utilizes a GDC electrolyte. At 600°C, Ceres Power reports 0.53 A cm<sup>-2</sup> at a cell voltage of 0.75 V.<sup>38</sup> It is expected that the slightly lower performance reported here of 0.85 A cm<sup>-2</sup> with the LSC/GDC cathode sintered ex situ and of 0.99 A cm<sup>-2</sup> with the LSC cathode activated in situ is a result of the electrochemically less active Ni/YSZ anode cermet compared to the Ni/doped ceria cermets. 16,18 This conclusion is supported by the high performance obtained at JÜLICH on anode-supported SOFCs,<sup>39</sup> in which the LSCF cathodes are subjected to higher sintering temperatures of more than 1000°C, thus resulting in a coarser (i.e. less active) microstructure.

## Conclusions

The present investigation was carried out in order to pursue the previous steps of improving the cathode fabrication of MSCs, thereby enhancing their reliability during cell operation. The results provide a significantly improved handling of entire cells sintered ex situ. The application of ex situ sintering to LSC-based cathodes was enabled

by utilizing the cathode as a dual-phase composite consisting of the perovskite material LSC and GDC as the second phase. Moreover, improved stability of the dual-phase cathode was achieved compared to pure LSCF cathodes sintered ex situ. Whereas LSCF cathodes sintered ex situ fail within a few days of storage in ambient air due to La(OH)<sub>3</sub> formation resulting in the spallation of the layer, LSC/GDC cathodes can be stored under ambient conditions without impeding their mechanical integrity. It was concluded that a rigid GDC network provides additional mechanical stability. Therefore, failure is prevented even when the LSC is decomposed and La(OH)3 is formed. During the first hours of cell operation, the initial cathode phase composition is restored by a reversible phase transformation, which occurs at  $T \ge 750$ °C in air. Electrochemical activity of the re-oxidized dual-phase cathode was proven in a single-cell measurement. At T < 750°C, the performance of the LSC/GDC dual-phase cathode was found to be higher than that of the pure LSCF cathode sintered ex situ, but lower than that of the LSC cathode activated in situ. Overall, a current density of 1.30 A cm<sup>-2</sup> at 750°C, 0.85 A cm<sup>-2</sup> at 700°C, and 0.54 A cm<sup>-2</sup> at 650°C was achieved at a cell voltage of 0.7 V for the LSC/GDC dual-phase cathode. For LSCF, current densities of 1.32 A cm<sup>-2</sup>, 0.82 A cm<sup>-2</sup>, and 0.49 A cm<sup>-2</sup> were obtained, whereas LSC achieved 1.37 A cm<sup>-2</sup>,  $0.99~A~cm^{-2}$ , and  $0.60~A~cm^{-2}$  at 0.7~V and operating temperatures of 750°C, 700°C, and 650°C, respectively. Electrochemical performance can be further enhanced through the application of improved cathodes on cells with Ni/GDC anodes, which are known to result in increased electrochemical activity. Furthermore, dual-phase cathodes might be enhanced by optimizing the cathode microstructure. Approaches for achieving this optimization include an adjustment of the LSC/GDC ratio, the particle sizes of the powders, and the cathode thickness as well as a specific adjustment of the sintering conditions to the dual-phase composition.

## Acknowledgments

The authors thank S. Hummel, T. Brambach, and C. Tropartz for conducting the electrochemical tests, Dr. Y. J. Sohn for conducting XRD measurements, and Dr. D. Sebold for SEM analysis. Furthermore, the authors would also like to thank the Austrian Federal Ministry for Digital and Economic Affairs (BMDW) as well as the industrial partners for providing the Christian Doppler Laboratory with funding.

# **ORCID**

D. Udomsilp https://orcid.org/0000-0002-4116-6141
N. H. Menzler https://orcid.org/0000-0001-7091-0980
A. K. Opitz https://orcid.org/0000-0002-2567-1885

#### References

- A. B. Stambouli and E. Traversa, "Solid oxide fuel cells (SOFCs): a review of an environmentally clean and efficient source of energy," *Renewable and Sustainable Energy Reviews*, 6, 433 (2002).
- W. Vielstich, Handbook of fuel cells. fundamentals, technology and applications / fundamentals and survey of sytems, New York, NY: Wiley, 2003.
- K. Eguchi, H. Kojo, T. Takeguchi, R. Kikuchi, and K. Sasaki, "Fuel flexibility in power generation by solid oxide fuel cells," *Solid State Ionics*, 152–153, 411 (2002).
- D. J. L. Brett, A. Atkinson, N. P. Brandon, and S. J. Skinner, "Intermediate temperature solid oxide fuel cells," *Chemical Society Reviews*, 37, 1568 (2008).
- V. V. Krishnan, "Recent developments in metal-supported solid oxide fuel cells," Wiley Interdisciplinary Reviews: Energy and Environment, n/a-n/a 2017.
- M. C. Tucker, "Progress in metal-supported solid oxide fuel cells: A review," *Journal of Power Sources*, 195, 4570 (2010).
- 7. P. Blennow, B. R. Sudireddy, Å. H. Persson, T. Klemensø, J. Nielsen, and K. Thydén, "Infiltrated SrTiO3:FeCr-based Anodes for Metal-Supported SOFC," *Fuel Cells*, n/a-n/a (2013)
- R. T. Leah, A. Bone, E. Hammer, A. Selcuk, M. Rahman, A. Clare et al., "Development Progress on the Ceres Power Steel Cell Technology Platform: Further Progress Towards Commercialization," *ECS Transactions*, 78, 87 (2017).
- B. J. McKenna, N. Christiansen, R. Schauperl, P. Prenninger, J. Nielsen, P. Blennow et al., "Advances in Metal Supported Cells in the METSOFC EU Consortium," *Fuel Cells*, 13, 592 (2013).

- J. Nielsen, A. H. Persson, T. T. Muhl, and K. Brodersen, "Towards High Power Density Metal Supported Solid Oxide Fuel Cell for Mobile Applications," ECS Transactions, 78, 2029 (2017).
- "MeStREx project uses ethanol fueled SOFCs in EV range-extenders," Fuel Cells Bulletin, 2016, 2 (2016).
- A. Ansar, P. Szabo, J. Arnold, Z. Ilhan, D. Soysal, R. Costa et al., "Metal Supported Solid Oxide Fuel Cells and Stacks for Auxiliary Power Units - Progress, Challenges and Lessons Learned," *ECS Transactions*, 35, 147 (2011).
- J. Rechberger and P. Prenninger, "The role of fuel cells in commercial vehicles," SAE Technical Papers, Commercial Vehicle Engineering Congress and Exhibition, 2007.
- D. Udomsilp, D. Roehrens, N. H. Menzler, C. Bischof, L. G. J. de Haart, A. K. Opitz et al., "High-Performance Metal-Supported Solid Oxide Fuel Cells by Advanced Cathode Processing," *Journal of The Electrochemical Society*, 164, F1375 (2017).
- T. Franco, M. Brandner, M. Rüttinger, G. Kunschert, A. Venskutonis, and L. Sigl, "Recent Development Aspects of Metal Supported Thin-Film SOFC," ECS Transactions, 25, 681 (2009).
- M. Haydn, C. Bischof, D. Udomsilp, A. K. Opitz, G. Bimashofer, W. Schafbauer et al., "Metal Supported SOFCs: Electrochemical Performance under Various Testing Conditions," ECS Transactions, 78, 1993 (2017).
- B. Tabernig, T. Franco, A. Venskutonis, H. Kestler, and L. Sigl, P/M FeCr alloy as interconnector and substrate materials for metal supported solid oxide fuel cells, 3, (2011).
- V. A. Rojek-Wöckner, A. K. Opitz, M. Brandner, J. Mathé, and M. Bram, "A novel Ni/ceria-based anode for metal-supported solid oxide fuel cells," *Journal of Power Sources*, 328, 65 (2016).
- M. C. Tucker, "Metal-Supported Solid Oxide Fuel Cell with High Power Density," ECS Transactions, 78, 2015 (2017).
- D. Udomsilp, "Charakterisierung und Optimierung der Grenzfläche Elektrolyt/Kathode in metallgestützten Festelektrolyt-Brennstoffzellen," 411, Schriften des Forschungszentrums Jülich Reihe Energie & Umwelt / Energy & Environment, Forschungszentrum Jülich GmbH Zentralbibliothek, Verlag, Jülich, 2018.
- M. Bram, D. Udomsilp, D. Roehrens, N. H. Menzler, A. K. Opitz, L. G. J. de Haart et al., "High Performance (La,Sr)(Co,Fe)O3 Cathodes with Improved Adherence for Metal-Supported Fuel Cells," *ECS Transactions*, 78, 709 (2017).
- D. Udomsilp, D. Roehrens, N. H. Menzler, A. K. Opitz, O. Guillon, and M. Bram, "Novel processing of La<sub>0.58</sub>Sr<sub>0.4</sub>Co<sub>0.2</sub>Fe<sub>0.8</sub>O<sub>3-δ</sub> cathodes for metal-supported fuel cells," *Materials Letters*, 192, 173 (2017).
- A. Venskutonis, G. Kunschert, E. Mueller, and H.-M. Hoehle, "P/M Processing and Coating Technologies for Fabrication of Interconnect for Stationary and Mobile SOFC Applications," ECS Transactions, 7, 2109 (2007).
- M. Haydn, K. Ortner, T. Franco, S. Uhlenbruck, N. H. Menzler, D. Stöver et al., "Multi-layer thin-film electrolytes for metal supported solid oxide fuel cells," *Journal of Power Sources*, 256, 52 (2014).
- S. P. Simner, J. F. Bonnett, N. L. Canfield, K. D. Meinhardt, J. P. Shelton, V. L. Sprenkle et al., "Development of lanthanum ferrite SOFC cathodes," *Journal of Power Sources*, 113, 1 (2003).
- S. P. Simner, J. F. Bonnett, N. L. Canfield, K. D. Meinhardt, V. L. Sprenkle, and J. W. Stevenson, "Optimized Lanthanum Ferrite-Based Cathodes for Anode-Supported SOFCs," *Electrochemical and Solid-State Letters*, 5, A173 (2002).
- C. Sun, R. Hui, and J. Roller, "Cathode materials for solid oxide fuel cells: a review," *Journal of Solid State Electrochemistry*, 14, 1125 (2010).
- H. Yokokawa, N. Sakai, T. Horita, K. Yamaji, M. E. Brito, and H. Kishimoto, "Thermodynamic and kinetic considerations on degradations in solid oxide fuel cell cathodes," *Journal of Alloys and Compounds*, 452, 41 (2008).
- A. Mai, V. A. C. Haanappel, S. Uhlenbruck, F. Tietz, and D. Stöver, "Ferrite-based perovskites as cathode materials for anode-supported solid oxide fuel cells: Part I. Variation of composition," *Solid State Ionics*, 176, 1341 (2005).
   T. Franco, M. Haydn, R. Mücke, A. Weber, M. Rüttinger, O. Büchler et al., "De-
- T. Franco, M. Haydn, R. Mucke, A. Weber, M. Ruttinger, O. Buchler et al., "Development of Metal-Supported Solid Oxide Fuel Cells," *ECS Transactions*, 35, 343 (2011).
- T. Franco, M. Haydn, A. Weber, W. Schafbauer, L. Blum, U. Packbier et al., "The Status of Metal-Supported SOFC Development and Industrialization at Plansee," *ECS Transactions*, 57, 471 (2013).
- M. Haydn, T. Franco, R. Mücke, M. Rüttinger, N. H. Menzler, A. Weber et al., "A Novel Manufacturing Route for Metal-Supported Thin-Film Solid Oxide Fuel Cells," in Euro PM 2012, 2012.
- M. Haydn, K. Ortner, M. Rüttinger, T. Franco, T. Jung, and S. Uhlenbruck, "Mehrlagige Schichtanordnung für einen Festkörperelektrolyt," ed: Google Patents, 2016.
- S. M. Gross, T. Koppitz, J. Remmel, J.-B. Bouche, and U. Reisgen, "Joining properties of a composite glass-ceramic sealant," Fuel Cells Bulletin, 2006, 12 (2006).
- F. Tietz, A. Mai, and D. Stöver, "From powder properties to fuel cell performance A holistic approach for SOFC cathode development," *Solid State Ionics*, 179, 1509 (2008).
- E. Dogdibegovic, R. Wang, G. Y. Lau, and M. C. Tucker, "High performance metalsupported solid oxide fuel cells with infiltrated electrodes," *Journal of Power Sources*, 410–411, 91 (2019).
- P. Blennow, T. Klemenso, A. Persson, K. Brodersen, A. K. Srivastava, B. R. Sudireddy et al., "Metal-Supported SOFC with Ceramic-Based Anode," *ECS Transactions*, 35, 683 (2011).
- R. T. Leah, A. Bone, E. Hammer, A. Selcuk, M. Rahman, A. Clare et al., "Development of High Efficiency Steel Cell Technology for Multiple Applications," *ECS Transactions*, 78, 2005 (2017).
- L. Blum, L. G. J. de Haart, J. Malzbender, N. H. Menzler, J. Remmel, and R. Steinberger-Wilckens, "Recent results in Jülich solid oxide fuel cell technology development," *Journal of Power Sources*, 241, 477 (2013).